View metadata, citation and similar papers at core.ac.uk

brought to you by CORE

provided by Ministry of Earth Sciences, Government of India

Author version: *Meteorol. Atmos. Phys., vol.109(3-4); 2010; 91-106*

Simulation of coastal winds along the central west coast of India using MM5 mesoscale model

Dhanya Pushpadas[a*] , P. Vethamony[a], K.Sudheesh[a], Smitha George[b], M. T. Babu[a] and Balakrishnan Nair T.M.[c]

[a] National Institute of Oceanography, Dona Paula, Goa 403 004, India

[b] Space Applications Centre, Ahmedabad, 380015, India

[c] Indian National Centre for Ocean Information Services, Hyderabad 500 055, India

* Dhanya Pushpadas

National Institute of Oceanography, Dona Paula, Goa 403 004, India

Email: dhanyapushpadas@gmail.com

Phone: +91 8322450541

Fax: +91 8322450608

Abstract

High resolution mesoscale model (MM5) has been used to study the coastal atmospheric circulation of central west coast of India, and Goa in particular. The model is employed with three nested domains. The innermost domain of 3km mesh covers Goa and the surrounding region. Simulations have been carried out for three different seasons – northeast (NE) monsoon, transition period and southwest (SW) monsoon with appropriate physics options to understand the coastal wind system. Simulated wind speed and direction match well with the observations. The model winds show the presence of sea breeze during the NE monsoon season and transition period, and its absence during the SW monsoon season. In the winter period, the synoptic flow is northeasterly (offshore) and it weakens the sea breeze (onshore flow) resulting in less diurnal variation, while during the transition period, the synoptic flow is onshore and it intensifies the sea breeze. During the northeast monsoon at an altitude of above 750 m wind direction reverses, and this is the upper return current, indicating the vertical extent of sea breeze. Well developed land sea breeze circulation occurs during the transition period, with vertical extension of 300 m and 1100 m, respectively.

1. Introduction

Coastal winds play a key role in controlling weather, transporting pollutants and generating several oceanic phenomena such as circulation and upwelling. Coastal wind circulation in the tropical region is dominated by thermally driven sea breeze-land breeze circulation, which is a mesoscale phenomenon that arises from the differential heating along the land-sea interface. Land breeze and sea breeze are more frequently and prominently observed in the tropical coastal region due to strong radiative heating, convection, and weak Coriolis force. It has been shown that direction (offshore, parallel, onshore) and strength of the synoptic flow affects structure and evolution of the sea breeze (Wexler 1946; Frizzola and Fisher 1963; Pielke 1974; Bechtold et al. 1991). The sea breeze system is also influenced by the prevailing large-scale wind, surface heating, latitude, and topographic friction (Atkinson 1981; Rotunno 1983; Yan and Anthes 1987; Atkins and Wakimoto 1997). The study of sea breeze finds applications in air pollution transport, location and initiation of convection, aviation safety, gliding and sailing, forest fire forecasting and impact on coastal processes (Simpson 1995; Lu and Turco 1994; Rao and Fuelberg 2000). For example, transport of pollutants in the marine boundary layer (MBL) depends on the extent and intensity of coastal wind circulation.

Several researchers have studied the sea breeze circulation theoretically and numerically (Haurwitz 1947; Mak and Walsh 1976; Arrit 1989; Dalu and Pielke 1989; Bechtold et al. 1991). Some of these studies focus on the effect of topography, land cover and vegetation on the land-sea breeze system and modelling of sea breeze circulation in a complex coastal environment (Cai and Steyn 2000; Sicardi et al. 2005). Franchito et al. (1998) confirmed that there is a positive feedback between sea breeze and coastal upwelling along the Cabo Frio coast, Brazil. Gilliam et al. (2004) indicated that the coastline shape and coast-relative flow direction are important factors in determining how the sea breeze circulation evolves spatially. Gille et al. (2003) used QuikSCAT data to determine a statistically significant signal along most of the world's coastline based on changes in wind direction between morning and evening, which is one of the characteristics of the sea-breeze system.

Sea breeze and land breeze circulation along certain regions of the Indian coast have been studied using numerical modelling and field data collected during INDOEX IP-99 (Subrahamanyam et al. 2001; Jamina and Lakshminarasimhan 2004; Simpson and Raman 2006; Srinivas et al. 2006; Srinivas et al. 2007). Sea breeze circulation was shown to be the dominant mechanism initiating rainfall over the east coast of India during the Indian southwest monsoon (Simpson et al. 2007). Aparna et al. (2005) presented an objective method for quantifying the seaward extent of sea breeze using QuikSCAT data.

Land-sea breeze, being a local circulation, is not captured in the operational weather observations; hence mesoscale modellling is essential to study its influence on various coastal processes. As fine resolution winds are required for many coastal studies along the Indian coast, this present study has been taken up in order to examine the aptness of a high-resolution mesoscale atmospheric model PSU/NCAR MM5 (Grell et al. 1994) for the simulation of coastal winds along the central west coast of India. The details of the model are described by Grell et al. (1994). MM5 has been increasingly used in operational numerical weather forecasting (Kotroni and Logouvardos 2004; Zhong et al. 2005) and air quality studies (Grell et al. 2000; Chandrasekar et al. 2003; Jackson et al. 2006; Mao et al. 2006). MM5 includes nested domains and necessary physics for convection, radiation and boundary layer turbulence. No study has been conducted using multi

day MM5 performance with higher resolution (a few km for horizontal resolution) over the central west coast of India. The primary objective of this numerical study is to validate the model for the central west of India for different seasons so that it can be used to provide fine resolution meteorological parameters to wave models and water quality models which are currently in operation at National Institute of Oceanography. Since mixing in the ocean is proportional to the third power of the wind speed, it is important to use fine resolution wind fields to force ocean models. The synoptic winds over India vary according to the prevailing northeast (NE) monsoon (October to February), southwest (SW) monsoon (June to September) and westerlies during pre-monsoon (March to May). In this paper, simulated coastal winds for the above three seasons are studied and the simulation results are validated with both offshore and inland observations. Further, characteristics such as onset, intensity, duration, and horizontal extent of land-sea breeze circulation off Goa have been analyzed. As land-sea breeze is a vertical circulation, in order to estimate the 'Return current' which is the compensatory flow for the thermally driven land-sea breeze circulation at higher altitudes, higher level winds were also analysed. This study also attempts to identify the synoptic wind patterns favoring the sea breeze - land breeze development along the central west coast of India. The aim of this study is to enhance the knowledge of coastal wind circulation, its onshore and offshore extent over central west coast of India.

2. Area of study and data used

Goa is situated on the central west coast of India and the coastline is oriented to approximately 340º□N. The terrain is, in general, sloping and hilly, and the elevation is about 20 m above MSL near the coast and increases to 600m above MSL towards 100km inland (Fig.1). Strand vegetation is prominent along the coastal belt with a corresponding roughness length of 1m. The study region frequently experiences the land-sea breeze circulation due to difference in land and sea temperature and large-scale geostrophic winds. Time series wind data were obtained from the moored shallow water buoy (SW3; location: 15º 23'N, 73º 44'E) and deep water buoy (DS1; location: 15º29'N, 69º16'E) deployed off Goa by the National Institute of Ocean Technology (NIOT), Chennai. The stated accuracies for wind speed and direction for NIOT buoys are ± 1.5% with resolution of 0.07m/s for wind speed and 0.1º for direction (Premkumar et al. 2000). Eight observations are obtained every day. Post calibration and error flagging of data are carried out by NIOT before the buoy data is released. Wind data have also been obtained from the Autonomous Weather Station (AWS) installed at Dona Paula, in proximity to the coast of Goa (15º 27'N, 73º 48'E). The height of the AWS is about 50m above sea level. The recorded data were ten-minute vector averages of wind speed and direction. Upper wind observations for the Goa region were obtained from the website http://weather.uwyo.edu/upperair/sounding.html.

3. Numerical model set-up

The non-hydrostatic Penn State/NCAR mesoscale model MM5 (Grell et al. 1994) is used for the present study. The model is employed with three nested domains (Fig.1) having horizontal grid resolutions of 27km, 9km, and 3km and 23 vertical levels. The outermost domain (27km mesh) covers the Indian Peninsula and Eastern Arabian Sea and the innermost domain (3km mesh) covers the Goa region (central west coast). Goa region has been selected for the following two reasons: (i) effect of land –sea breeze system is strongly experienced and (ii) time series AWS and buoy data are available for validation of model results. The model has a number of options for physical processes for radiation, convection, atmospheric boundary layer and surface processes. The present study offered the most desirable physics

options for the model after studying the sensitivity of different schemes using observations at various stations in Goa region. For PBL parameterization, MRF scheme is used in the model. It is a non-local first-order scheme in which the vertical transfers are dependent on the bulk characteristics of the PBL, and include counter gradient transports of temperature and moisture that account for the contributions from large-scale eddies. The eddy diffusivity coefficient for momentum is a function of the friction velocity and the PBL height, while those for temperature and moisture are computed using a Prandtl number relationship. Details of the model domains, grid cell size, parameterization scheme used for atmospheric boundary layer, convection, radiation and surface physics are given in Table 1.

The surface temperature is predicted using a Five Layer Soil Model (Dudhia 1996). Grell scheme is employed for cumulus parameterization (Grell 1993), and Simple Ice explicit scheme for moisture (Dudhia 1989). The National Center for Environmental Prediction (NCEP) global final analyses data (FNL 6 hourly and 1^0x1^0) is used to initialize the model, and provide continuous lateral and lower boundary conditions. This contains horizontal and vertical winds, sea level pressure, surface pressure, temperature, specific humidity, geopotential height, soil moisture, soil temperature, sea surface temperature, skin temperature, precipitable water, etc. The model is initialized at 0000 UTC on each of the selected days and integrated for the next five days. The lateral and bottom boundary conditions in the model are updated at 6 h intervals. The forecast variables include the three wind components (u, v, w), air temperature, atmospheric moisture, turbulence kinetic energy (TKE), vorticity, divergence, precipitation, etc. among a host of meteorological parameters. The surface boundary values for terrain height, albedo, moisture availability, emissivity, roughness coefficient and thermal diffusivity of soil are specified from USGS data, and interpolated to the model grids. The USGS data are specified at 19km, 4km and 0.9km resolution for 27km, 9km and 3km grid meshes, respectively. Atmospheric radiation and cooling rates are calculated every 30 min using RRTM long wave scheme. Nested domains with two way interaction are used for the simulation. For the intermediate and innermost domains, the meteorological fields are interpolated from the coarse mesh, but terrain and land-use data are replaced with higher resolution fields from its own mesh. The default value of roughness length over ocean (z_0) is changed to tune up the model and the value is calculated based on Charnock relationship (Charnock 1955).

$$z_0 = a\,\tau / \rho_a g$$

where, τ is the total stress, ρ_a is the air density, a (=0.0185) is the Charnock parameter and g is acceleration due to gravity.

The synoptic wind is dominated by monsoon winds. It varies according to the southwest (SW) monsoon (June to September), northeast (NE) monsoon (October to February) systems and the transition period (March to May) predominantly as westerlies. These synoptic flow situations are relevant to the development of land-sea breeze circulation. Earlier studies showed that sea breeze along the Goa coastal region exists during the northeast monsoon and the transition period only, and during the southwest monsoon season, the wind field is dominated by the large-scale atmospheric circulation and there is practically no existence of land or sea breeze when the SW monsoon is active.

The simulation was carried out for the period 8-13 January 2006, 10-15 March 2006 and 15-20 July 2006, representing winter monsoon (northeast), transition between winter and summer monsoons and summer monsoon (southwest), respectively. The period of simulation is chosen in such a way that measured data should be available for validation of model results and well developed land-sea breeze circulation with its diurnal characteristics should be present. The

forecast variables include many meteorological parameters. Since both the buoy and AWS observations are of 10 minute and 3h intervals respectively, the model output is saved every hour so that the interval lies between both observations and also captures the diurnal characteristics of the variables well. The observed winds were reduced to 10 m winds using the equation of Liu et al. (1979). Early calculations showed that the wind speed errors using above equation were less that 2%. The model was initialized at 00UTC of 8 January, 10 March and 15 July 2006 and integration carried out for 5 days. But, for the present analysis, the horizontal components of winds at 10m height, surface temperature and relative humidity and upper layer horizontal wind components were extracted.

4. Results and discussions

The MM5 model incorporates most of the atmospheric dynamics and physics, and is suitable for the simulation of synoptic winds. While analyzing the nested model simulation, significance is mainly attached to the results of the innermost nest. However, as outer domain simulations influence the results of inner domain, and outer domain covers a wider perspective of the thermally induced coastal circulations, the results of the outermost nest are also discussed briefly. The present section describes the statistical analysis carried out for hourly simulations of MM5 surface winds along and very near to the Goa coastal region for three different seasons and observed wind data from AWS, available for the same period. The results are summarised in Table II. The statistical parameters evaluated are: (i) bias, (ii) standard deviation; (iii) the root mean square error (RMSE) and (iv) correlation coefficient between the observed and simulated hourly wind speeds. It may be noted that model values are in 3 km grid size and observations are point measurements. Hence, the bias between both the data sets as shown in Table II. Yet, the model has reproduced the average features and patterns of the hourly wind vector. This statistical analysis also showed that MM5 performance is more coherent when the mesoscale circulation dominates over the synoptic flow. The simulation results and circulation features of different seasons are discussed below.

4. 1. Circulation features during the northeast monsoon

Simulation for the winter season (NE monsoon) was carried out when the prevailing synoptic wind was northeasterly and offshore in the study region. The strength of the large scale wind ranges between 2 and 4 m/s. The simulated surface wind in the morning hours in the outermost domain is northeasterly and speed is of the order of 2-3 m/s {Fig. 2(a)}. It is difficult to differentiate the land breeze in this case as it is masked by the prevailing synoptic wind. The flow shifts to westerly at 1130 h indicating onset of sea breeze (not shown). This flow becomes stronger (>4 m/s) and moves northwesterly over land after 1330 h (Fig. 2b), indicating sea breeze circulation. The onset timing and extent of sea breeze circulation is clear in the simulation carried out for the innermost domain covering Goa region (Fig. 3). The westerly flow gains its maximum speed around 1630 h. The extent of sea breeze is about 120 km by 1630 h. It spreads inland 50 to 80 km from the coast. This result agrees with earlier studies carried out using QuikSCAT data and observations (Aparna et al 2005; Subrahmanyam et al. 2001). The simulation shows that sea breeze strikes the coast in a northwest-west direction. Apart from the change in direction, the onset of sea breeze can be understood from the gain in wind speed in the afternoon hours. During late night hours, wind direction along the coast changes and it becomes parallel to the coast indicating dissipation of sea breeze.

Model results (surface winds at 10m level at Goa) of the innermost domain are used for comparison with observations. Fig. 4 shows comparison of simulated surface wind and AWS observations. While the simulated onshore velocity component (u_{10}) and direction very closely match with the observations (Fig. 4a&d), the simulated alongshore velocity component (v_{10}) and wind speed (Fig. 4b&c) show deviation from the observations. This deviation of simulated v_{10} wind speeds could be due to (i) polarization of observed winds in the alongshore direction because of blocking effect of western Ghats and (ii) limitation of the model to catch topographic control very near to the coast (Stanton 1998). Furthermore, Halliwell and Allen (1987) explained that coastal mountain blocking can cause wind measurements to be strongly polarized in the alongshore direction. The model slightly under-estimates the higher values and overestimates the lower values of the observations. In the afternoon hours, the wind gains speed due to sea breeze circulation, and this can be explained based on u_{10} velocity component (Fig. 4a) and direction change (Fig. 4d). Simulated air temperature and relative humidity follow the trend of observed values even though the model underestimates the peak values {Fig. 4(e&f)}. As the sea breeze front passes, the relative humidity drops first, and then increases rapidly (Fig. 4f). Fig. 5 shows comparison of simulated surface wind and moored buoy (shallow water buoy, SW3, deployed off Goa) observations. The buoy observations are three hourly averages. The discontinuity in observed values indicates no data points at the particular time. As in the previous comparison, while simulated onshore velocity component (u_{10}) (Fig. 5a) and direction (Fig. 5d) closely match with the buoy observations, alongshore velocity component (v_{10}) (Fig. 5b) and wind speed (Fig. 5c) show deviation from the observations. These results also show the sea breeze characteristics: gain in wind speed in the afternoon hours and change in direction from morning to evening. During this period, the synoptic flow is northeasterly (offshore) and it weakens the sea breeze (onshore flow), resulting in less diurnal variation.

The model results from the inner domain are examined in detail to study the vertical wind profile of the Goa region. Vertical profiles of simulated and observed winds at 00UTC (0530 h) and 1200 UTC (1730h) on 12 January 2006 are shown in Fig. 6. Simulated wind matches well with observations. In the morning hours the winds are northeasterly and offshore, and the direction does not vary with altitude(Fig. 6b); however, in the afternoon hours (development of sea breeze), at a height of above 750m, wind direction reverses and this is the upper return current (sea breeze aloft Fig. 6d). Thus, the vertical extent of sea breeze during the northeast monsoon period is ~750m. From Fig. 6, it is evident that during NE monsoon, there exists a low-level sea breeze system and an upper level return current system from land to sea.

4. 2. Circulation features during the transition period

The simulation was performed from 10 to 15 March 2006, when the prevailing synoptic wind was northwesterly and onshore in the study region. The strength of the large scale wind was 3-5 m/s. The simulated surface wind in the morning hours in the outermost domain is northeasterly (~3m/s) on the west coast (not shown). It becomes westerly at 1230 h, indicating onset of sea breeze. This flow becomes stronger and northwesterly over land after 1400h. The circulation features are very clear from the simulation results of innermost domain (Fig. 7). In the morning hours, flow direction is northeast to east. The onset of land breeze (offshore) can be easily differentiated since the synoptic flow is onshore (Fig. 7a). An organized flow from sea to land in the northwesterly to westerly direction is established after 1030h. This flow becomes stronger after 1430h, and reaches upto 5m/s in the evening hours (Fig. 7c). The extent of sea breeze is about 160km by 1630h. The inland penetration of sea breeze obtained in the present numerical study matches with the experimental studies conducted at various locations all over the world (Buckley and Kurzeja 1997; Kottmeier et al.

2000). The simulation shows that surface winds are onshore about 60% of the daytime. The sea breeze strikes the coast in the northwesterly direction. It is difficult to differentiate the sea breeze in this case as it is masked completely by the prevailing synoptic wind. However, the onset time of sea breeze can be understood from the gain in wind speed at the coast as well as from direction. Late in the night, wind direction reverses to northeasterly along the coast which is an indication of well developed land breeze during this period (Fig. 7d).

Fig. 8 shows comparison of simulated surface winds, air temperature and relative humidity with AWS observations during the simulation period. As is the case in winter, here also simulated onshore velocity component (u_{10}) and direction closely follow the observations, while the simulated alongshore velocity component (v_{10}) and wind speed show deviations from the observation, but the deviation is small compared to that of the northeast monsoon. Diurnal variation, which is a characteristic of land-sea breeze system, is well developed during this period as is evident in the direction plot (Fig. 8d). Also, the wind speed during afternoon hours is higher than in winter. This is because of the intensification of sea breeze strength by the prevailing synoptic flow, which is also onshore. Simulated air temperature and relative humidity also follow the trend of observed values even though the model underestimates the higher values {Fig. 8(e&f)}.

Comparison of vertical profiles of simulated and observed winds at 00UTC (0530 h) and 1200 UTC (1730 h) on 12 March 2006 is shown in Fig. 9. Simulated wind follows the trend of observations. In the morning hours, the winds are northeasterlies and offshore (well developed land breeze) and at a height of 300m wind direction reverses to the upper return current (land breeze aloft) (Fig. 9b). In the afternoon hours, winds are well developed northwesterlies and onshore and at a height of 1100m wind direction reverses due to the significance of upper return current (sea breeze aloft, Fig. 9d) . So the vertical extent of sea breeze during the transition period is ~1100m and that of land breeze is ~300m. It is clear that a well developed land-sea breeze circulation occurs during the transition period. Even though there prevails a sea breeze circulation during northeast monsoon, its strength and, horizontal and vertical extends of land-sea breeze circulation are higher during the transition period.

4. 3. Circulation features during southwest monsoon

The simulation for the south-west monsoon season was performed from 15 to 20 July 2006 when the prevailing synoptic wind was westerly and onshore in the study region. In this case, wind speeds are dominated by large scale atmospheric circulation. There is no land or sea breeze when the monsoon is active. Simulated surface winds of outer domain (not shown) shows strong south westerly winds from the ocean to the continent. Previous studies reported that during summer monsoon (June to August) a low level atmospheric jet, known as Findlater jet with a broad region of strong southwesterly winds with remarkable steadiness in direction and strength blows from ocean to continent. Simulated surface winds from the innermost domain also show strong winds (~10m/s) during this period (Fig. 10).

Fig. 11 shows comparison of simulated surface wind, air temperature and relative humidity with AWS observations. In this case, simulated winds almost follow the observations. The speed and direction are maintained almost the same during the whole day which indicates the absence of sea breeze circulation. Fig. 12 shows comparison of simulated surface winds and observations of moored buoy DS1, deployed off Goa. As in the AWS comparison for the same period, in this case also simulated winds almost match with the observations. Simulation results show the absence of sea breeze

circulation during the south-west monsoon. During the monsoon period, the coast is dominated by large scale atmospheric circulation and the winds are onshore along the west coast of India.

Comparison of vertical profiles of simulated and observed winds at 00UTC (0530 h) on 17 July 2006 is shown in Fig. 13. Afternoon observations were not available for the same day. During this period, direction is nearly the same for surface and upper air. This is due to the absence of mesoscale circulation (land- sea breeze) during this period.

5. Conclusions

High resolution mesoscale simulations with the PSU/NCAR MM5 model were performed to study the coastal atmospheric circulation of the west coast of India, and Goa region in particular. MM5 model results were compared with AWS and moored buoy measurements. The study provided a successful multi-day simulation of coastal wind circulation for three different seasons. Onshore and alongshore wind components show diurnal variation which are due to land-sea breeze circulation. The seaward extent of the onshore (sea breeze) flow estimated from the simulation agrees with earlier studies. Statistical analyses provided an intangible indication of model's ability to reproduce the observed circulation characteristics of the coastal winds. The results show that MM5 is able to simulate magnitude, direction, timing and vertical extent of the coastal atmospheric circulation accurately. However, more analyses are needed to study the influence of the coastal winds with the complex terrain. It is proposed to couple MM5 model with other hydrodynamic models in order to study coastal waves, wind induced coastal circulation and oil spill dispersion of the west coast of India.

Acknowledgements

We thank Director and other scientists of INCOIS, Hyderabad for funding the project and Director, NIO, Goa for providing facilities at NIO. Author, Dhanya acknowledges CSIR for her fellowship. We are grateful to Mr. A.M. Almeida and Mr. Gaurish Salgaonkar of NIO for their help in setting up the new workstation for installing the MM5 model and Mr. Syam Shankar of NIO for his help in using GrADS software. Shri. S.G. Prabhudesai and his team is acknowledged for providing the AWS data. This is NIO contribution number xxxx.

References

Aparna M, Shetye SR., Shankar D, Shenoi SSC, Mehra P, Desai RGP (2005) Estimating the seaward extent of sea breeze from QuikSCAT scatterometry. Geophys Res Lett 32: L1360. doi:10.1029/2005GL023107

Arrit RW (1989) Numerical modelling of the offshore extent of the sea breezes. Quart J Met Soc. 115: 547-570

Atkins N, Wakimoto RM (1997) Influence of the synoptic-scale flow on sea breeze observed during Cape. Mon Wea Rev 125: 2112-2130

Atkinson BW (1981) Mesoscale Atmospheric Circulations. Academic Press, London

Bechtold P, Pinty J, Mascart P (1991) A numerical investigation of the influence of large-scale winds on sea-breeze and inland-breeze type circulations. J Appl Meteorol 30: 1268-1279

Buckley RL, Kurzeja RJ (1997) An observational and numerical study of the nocturnal sea breeze part I: structure and

circulation. J Appl Meteorol 36: 1577-1598

Cai XM, Steyn DG (2000) Modelling study of sea breezes in a complex coastal environment. Atmos Environ 34: 2873-2885

Chandrasekar A, Philbrick CR, Clark R, Doddridge B, Georgopoulos P (2003) Evaluating the performance of a computationally efficient MM5/CALMET system for developing wind field inputs to air quality models. Atmos Environ 37: 3267-327

Charnock H (1955) Wind Stress on water surface. Quart J Roy Met Soc 81: 639-640

Dalu GA (1989) An analytical study of sea breeze. J Atmos Sci 46: 1815-1825

Dudhia J (1989) Numerical study of convection observed during the winter monsoon experiment using a mesoscale two-dimensional model. J Atmos Sci 46: 3077-3107

Dudhia J (1996) A multi-layer soil temperature model for MM5. Preprints, The Sixth PSU/NCAR Mesoscale Model Users' Workshop, Boulder, Colorado, 49-50

Frechito SH, Rao VB, Stech JL., Lorenzetti JA (1998) The effect of coastal upwelling on sea breeze circulation in Cabo Frio Brazil :a numerical experiment. Ann Geophys 16: 866-881

Frizzola JA, Fisher RL (1963) A series of sea breeze observations in the New York City area. J Appl Meteorol 2: 722 - 739

Gille ST, Llewellyn Smith SG, Lee SM (2003) Measuring the sea breeze from QuikSCAT scatterometry. Geophys Res Lett 30(3) 1114: doi:10.1029/2002GL016230

Gilliam RC, Raman S, Devdutta S Niyogi (2004) Observational and numerical study on the influence of large scale flow direction and coastline shape on sea breeze evolution. Bound-Lay Meterol 111: 275-300

Grell GA (1993) Prognostic evolution of assumptions used by cumulus parameterizations. Mon Wea Rev 121: 764-787

Grell GA, Dudhia J, Stauffer DR (1994) A description of the fifth-generation Penn State/NCAR mesoscale model (MM5). NCAR Technical Note. NCAR/TN-398+STR, 117

Grell GA, Emies S, Stockwell WR, Schoenemeyer T, Forkel R., MIchealakes J, Knoche R., Seidl W. (2000) Application of a multiscale, coupled MM5/chemistry model to the complex terrain of the VOTALP valley campaign. Atmos Environ 34: 1435-1453

Halliwell GR, Allen JS (1987) The large-scale coastal wind field along the west coast of North America, 1981-1982. J Geophys Res 92: 1861-1884

Haurwitz B (1947) Comments on sea breeze circulation. Journal Meteorol 4(1): 1-8

Jackson B, Chau D, Gurer K, Kaduwela A (2006) Comparison of ozone simulations using MM5 and CALMET/MM5 hybrid meteorological fields for the July/August 2000 CCOS episode. Atmos Environ 40: 2812-2822

Jamina P, Lakshminarasimhan J (2004) Numerical Simulation of sea breeze characteristics observed at tropical coastal site, Kalpakkam. India. J Earth Sys Sci 113(2): 197-209

Kotroni V, Lagouvardos K (2004) Evaluation of MM5 high resolution real time forecasts over the urban area of Athens, Greece. J Appl Meteorl 43: 1666-1678

Kottmeier C, Palacio-Sese P, Kalthoff N, Corsmeiser U, Fiedler F (2000) Sea breezes and coastal jets in southern Spain. Int J Climatol 20:1791-1808

Liu WT, Kristina BK, Joost AB (1979) Bulk parameterization of air-sea exchanges of heat and water vapour including the molecular constraints at the interface. J. Atmos Sci 36: 1722-1735

Lu R, Turco RP (1994) Air pollutant transport in coastal environment. Part 1: Two dimensional simulations of sea breeze and mountain effects. J Atmos Sci 51: 2285-2308

Mak MK, Walsh JE (1976) On the relative intensities of sea and land breezes. *J* Atmos Sci 33: 242- 251

Mao Q, Gautney LL, Cook TM, Jacobs ME, Smith SN, Kelsoe JJ (2006) Numerical experiments on MM5-CMAQ sensitivity to various PBL schemes. Atmos Environ 40: 3092-3110

Neetu S, Shetye SR, Chandramohan P (2006) Impact of sea breeze on wind-seas off Goa, west coast of India. J Earth Sys Sci 115: 229-234

Pielke RA (1974) A three-dimensional numerical model of the sea breezes over south Florida. Mon Wea Rev 102: 115-139

Premkumar K, Ravichandran M, Kalsi SR, Sengupta D, Gadgil S (2000) First result from a new observational system over the Indian Seas. Curr Sci 78: 323-330

Rao PA, Fuelberg E (2000) An investigation of convection behind the Cape Canaversal Sea-Breeze front. Mon Wea Rev 128: 3437-3458

Rotunno R (1983) On the linear theory of the land and sea breeze. J Atmos Sci 40: 1999-2009

Sicardi V, Galmarini S, Riccio A, Steyn D (2005) Simulation of Land-sea Breeze Circulation on Sardinia Island using MM5 Mesoscale Model. Conference Proceeding 2005 1st Conference on Harbours and Air Quality, Genova, 15th-17th June 2005

Simpson JE (1995) Sea breeze and Local wind. Cambridge University Press, New York

Simpson M, Hary Warrior, Sethu Raman, Aswathanarayana PA, Mohanty UC, Suresh R (2007) Sea-breeze initiated rainfall over the east coast of India during the Indian southwest monsson. Nat Hazards 42: 401-413

Srinivas CV, Venkatesan R, Somayaji KM, Bagavat Singh A (2006) A numerical study of sea breeze circulation observed at a tropical site, Kalpakkam on the east coast of India under different synoptic flow situations. J Earth Sys Sci 115(5): 1-18

Srinivas CV, Venkatesan R, Bagavat Singh A (2007) Sensitivity of mesoscale simulations of land-sea breeze to boundary layer turbulence parameterization. Atmos Environ 41: 2534-2548

Stanton BR (1998) Ocean surface winds off the west coast of New Zealand: A comparison of ocean buoy, ECMWF model, and land based data. J Atmos Oceanic Technol 15:1164-1170

Subrahamanyam DB, Sen Gupta K, Sudha Ravindran, Praveena Krishnan (2001). Study of sea breeze and land breeze along the west coast of Indian sub-continent over the latitude range 15ºN to 8ºN during INDOEX IFP-99 (SK-141) cruise. Curr Sci 80: 85-88

Wexler R (1946) Theory and observations of land and sea breezes. Bull Am Meteorol Soc 27: 272-287

Yan H, Anthes RA (1987) Effect of latitude on the sea breeze. Mon Wea Rev 115: 936-956

Zhong, SY, In HJ, Bian, XD, Charney J, Heilman W, Potter B (2005) Evaluation of real-time high resolution MM5 predictions over the Great Lakes Region. Weath Forecast 20: 63-81

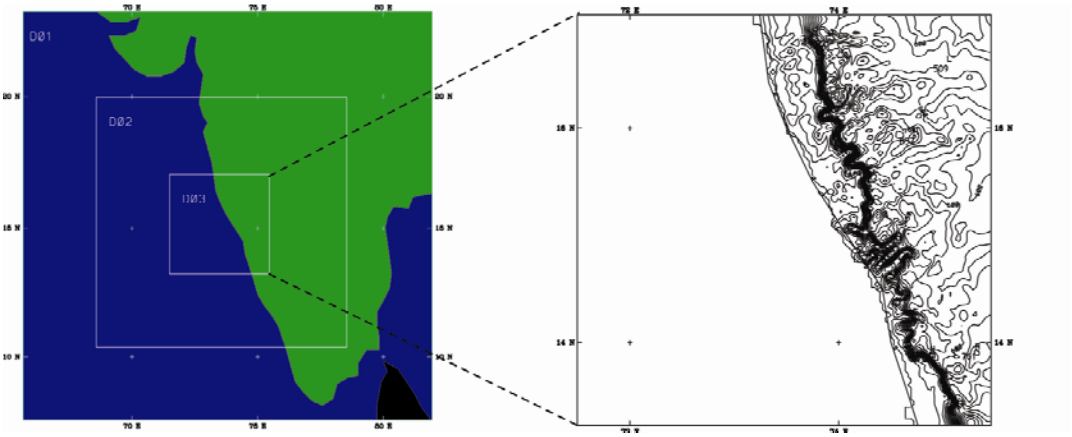

Fig. 1 Domains used in MM5 model (left panel). The inset figure in the right panel shows the innermost domain covering Goa and surrounding region with topographic details where the elevation contours are drawn at 50m interval

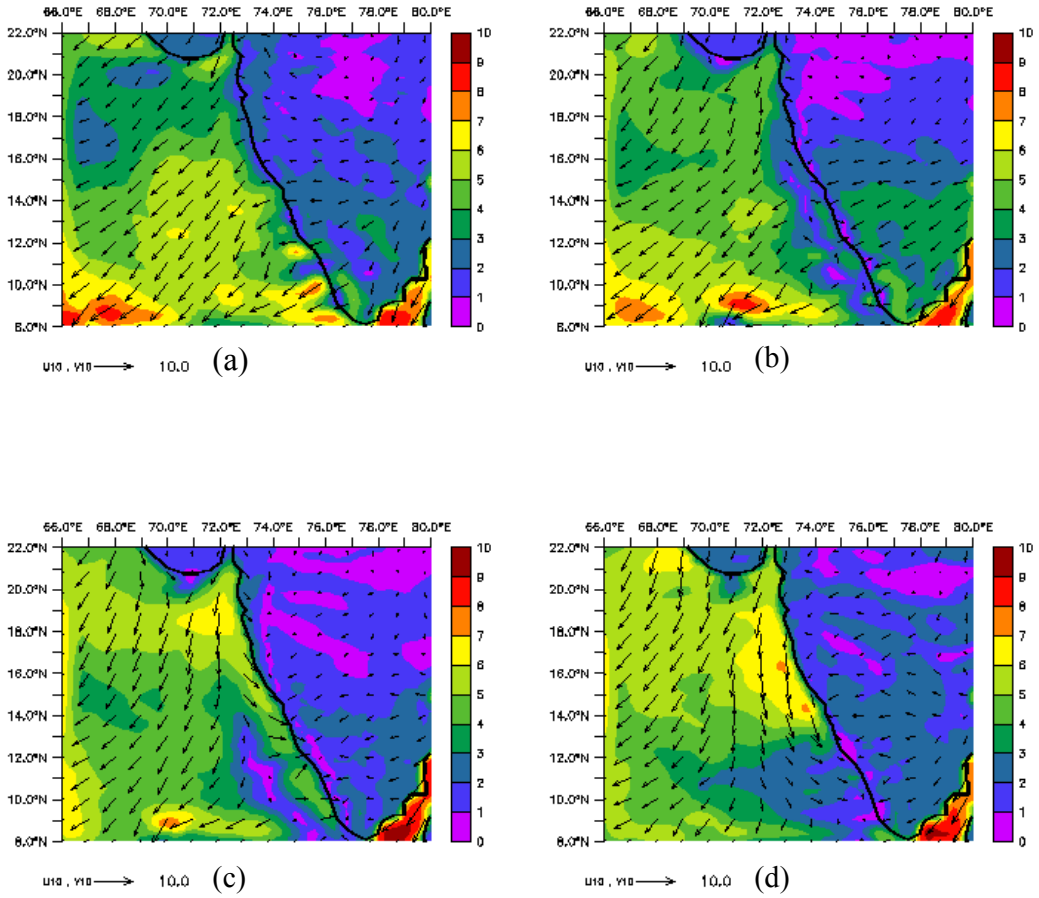

Fig. 2 Simulated surface winds of outer domain at (a) 0530 h, (b) 1330 h, (c) 1730 h and (d) 2130 h (IST) on 10 January 2006

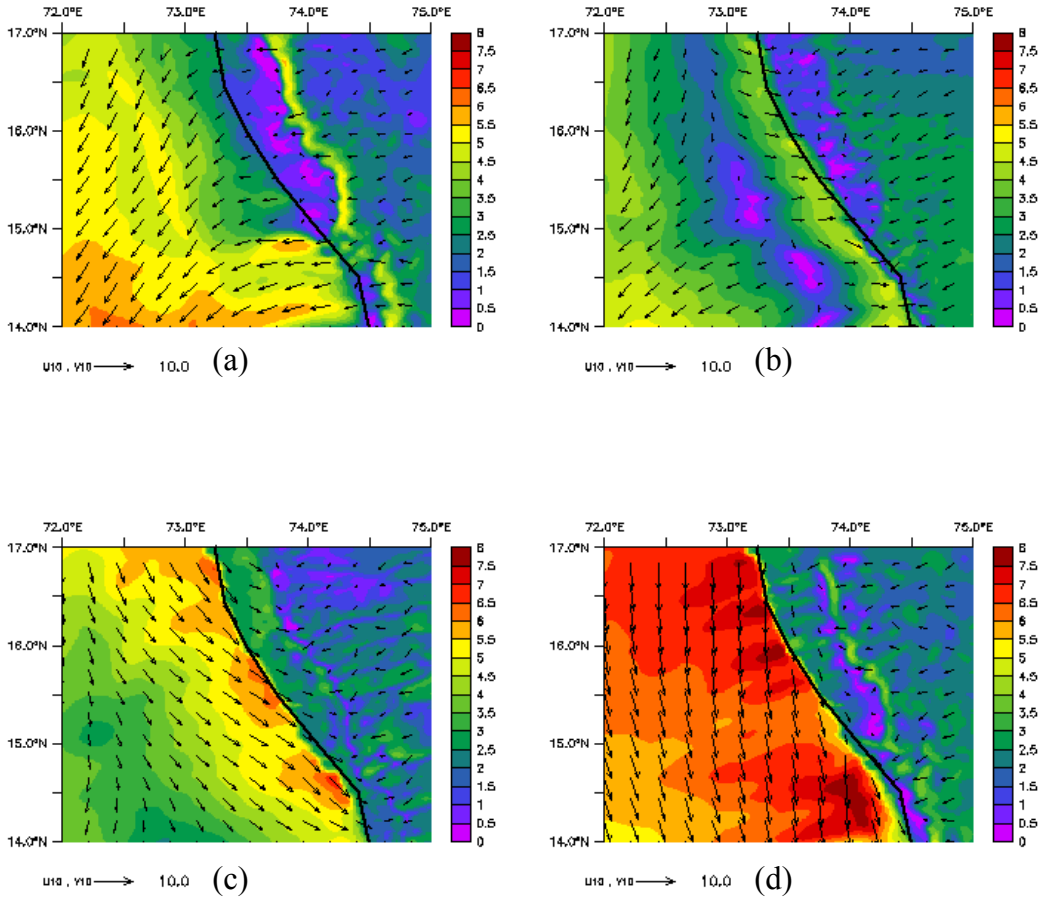

Fig. 3 Simulated high resolution surface winds in the Goa region at (a) 0530 h, (b))1330 h, (c) 1730 h and (d) 2130 h (IST) on 10 January 2006

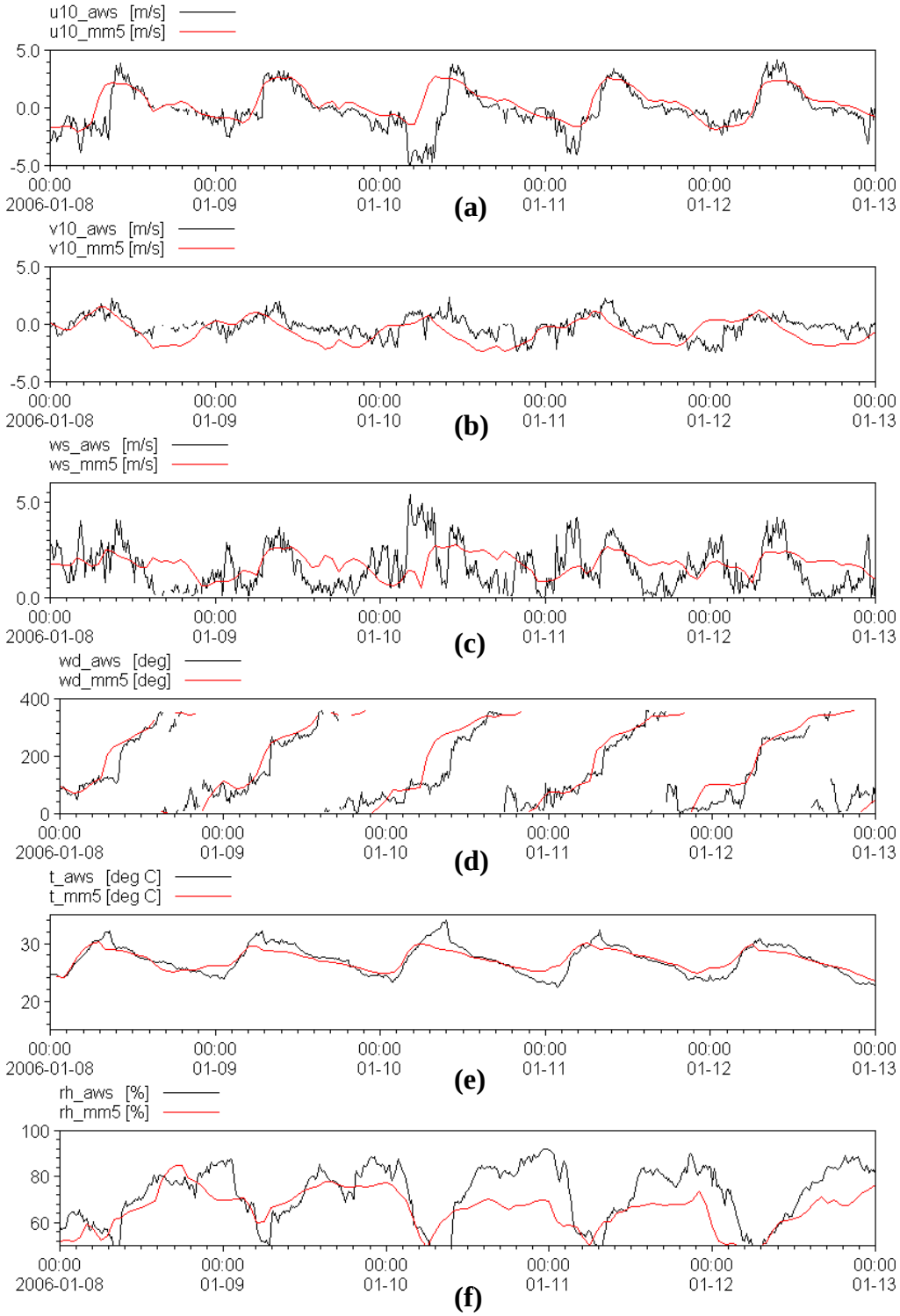

Fig. 4 Comparison of simulated and AWS observed (a) u-velocity component at 10m height, (b) v-velocity component at 10m height, (c) wind speed (d) wind direction, (e) air temperature and (f) relative humidity (time in UTC) of January 2006

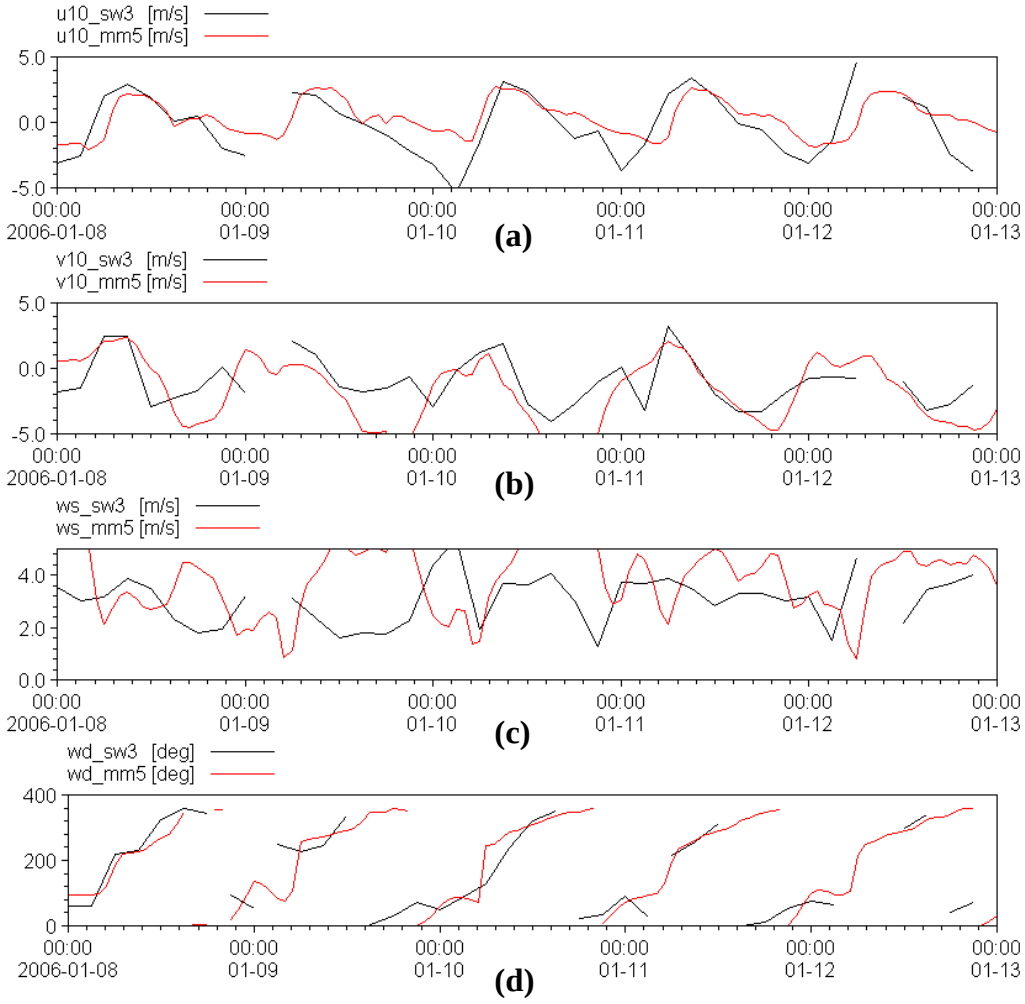

Fig. 5 Comparison of simulated and moored buoy (SW3) observations: (a) u-velocity component, (b) v-velocity component, (c) wind speed and (d) wind direction (time in h) of January 2006

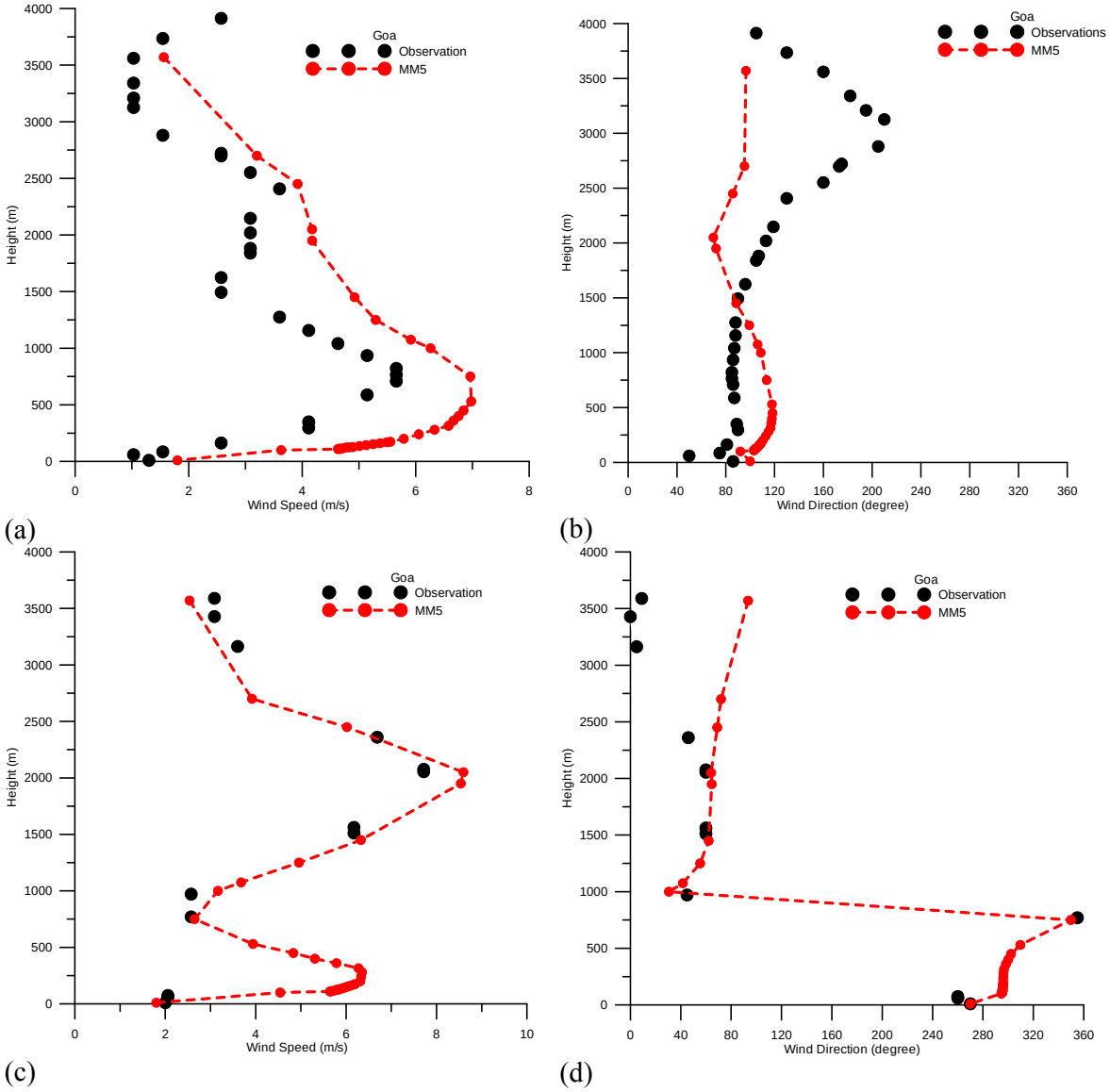

Fig. 6 Comparison of simulated and observed vertical profile of (a)wind speed at 00GMT, (b)wind direction at 00 GMT, (c) wind speed at 1200GMT and (d) wind direction at 1200GMT of 12 January 2006

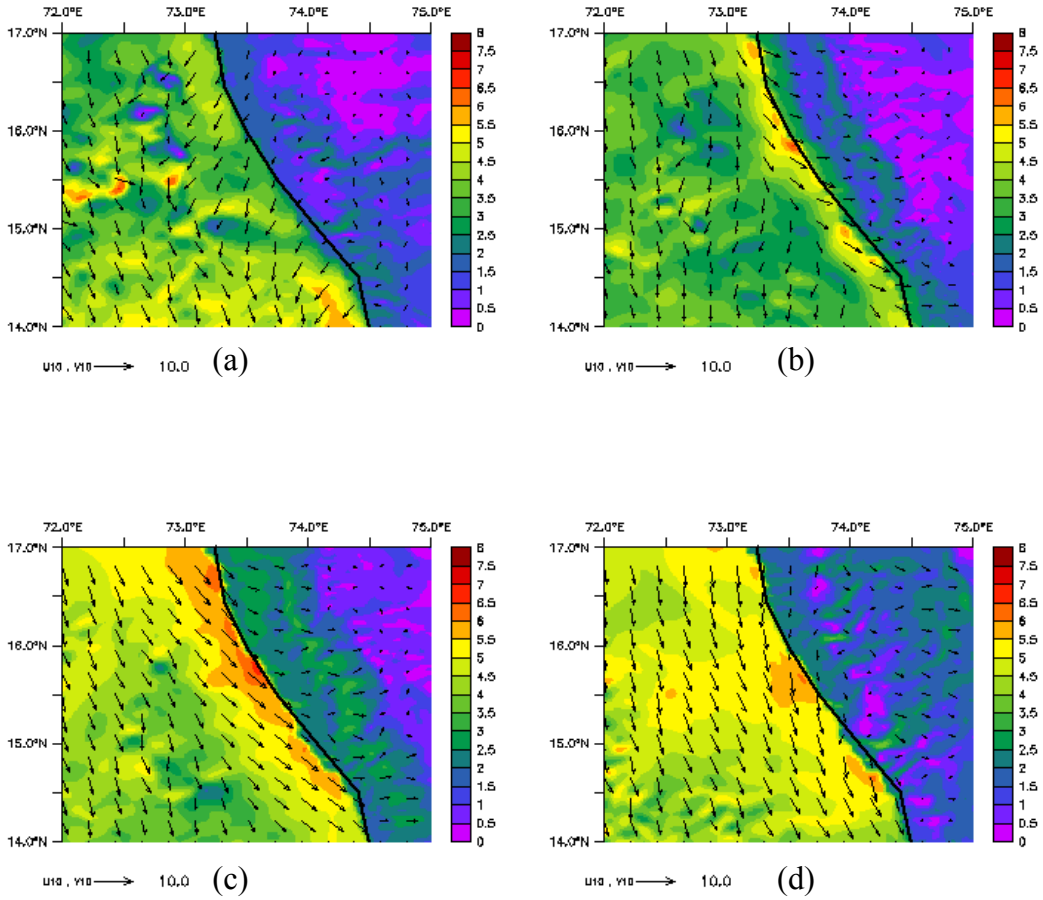

Fig. 7 Simulated high resolution surface in the Goa region at (a) 0530 h, (b) 1330 h, (c) 1730 h, and (d) 2130 h respectively on 12 March 2006

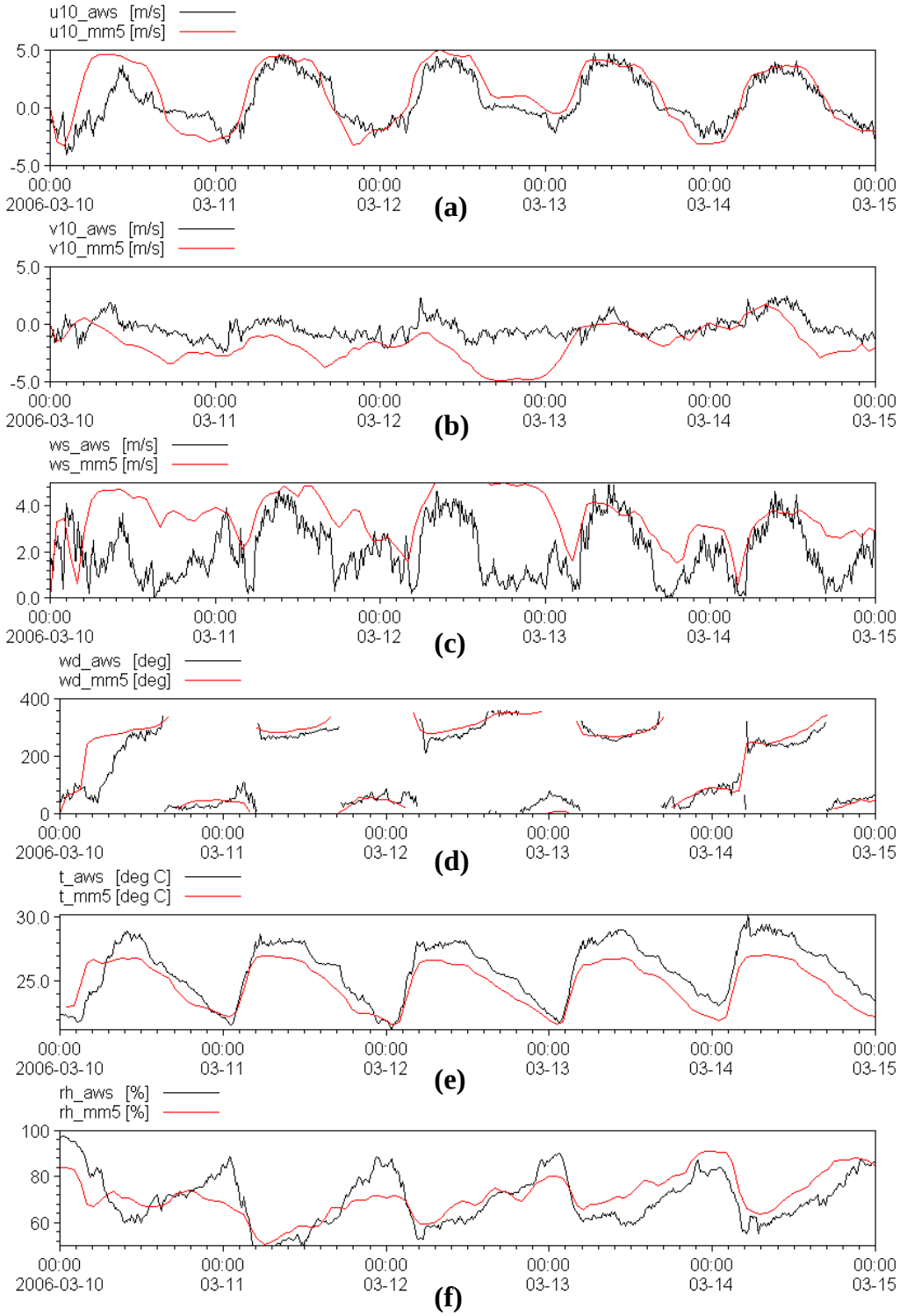

Fig. 8 Comparison of simulated and AWS observed (a) u-velocity component at 10m height, (b) v-velocity component at 10m height, (c) wind speed (d) wind direction, (e) air temperature and (f) relative humidity (time in UTC) of March 2006

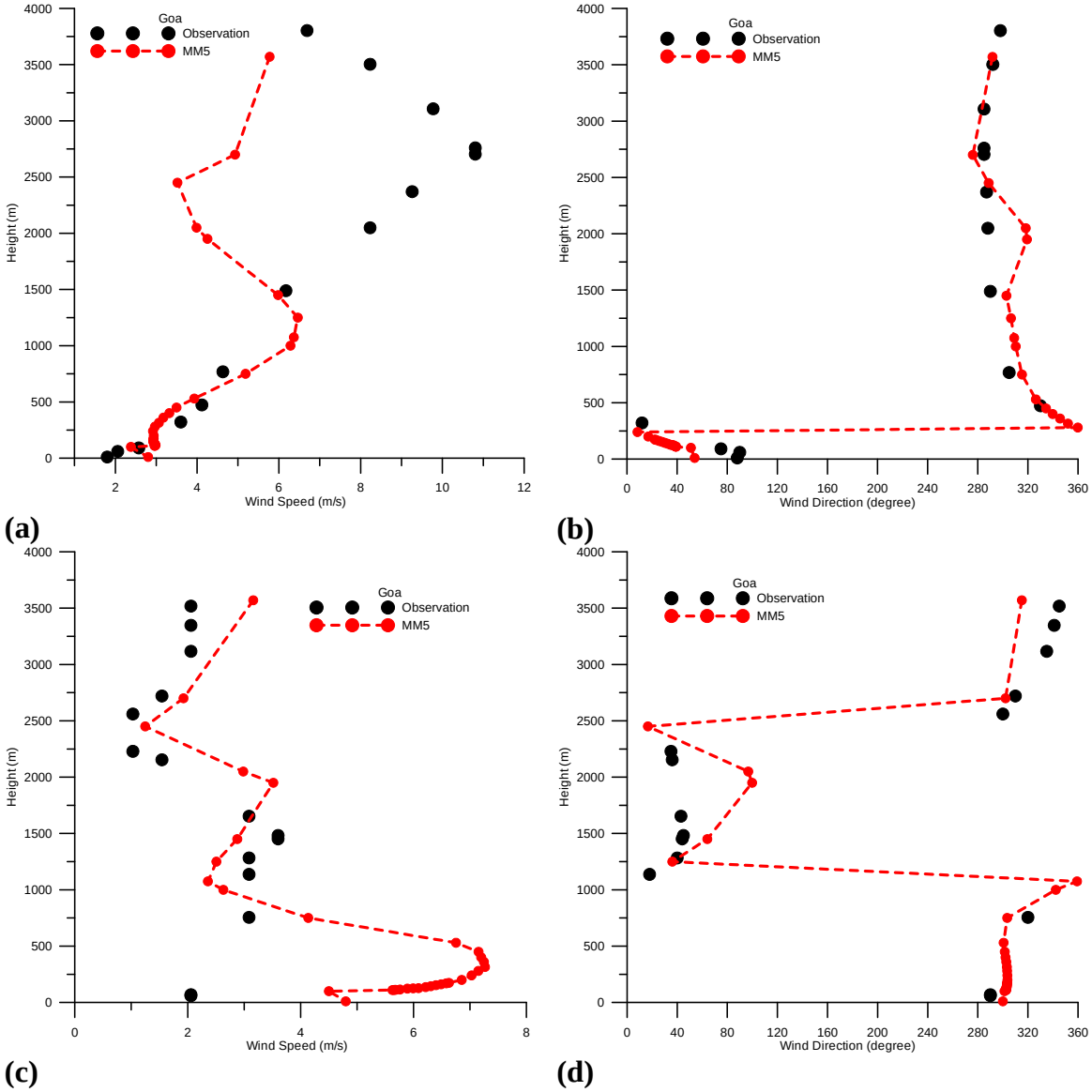

Fig. 9 Comparison of simulated and observed vertical profile of (a) wind speed at 00GMT, (b)wind direction at 00 GMT, (c) wind speed at 1200GMT and (d) wind direction at 1200GMT of 12 March 2006

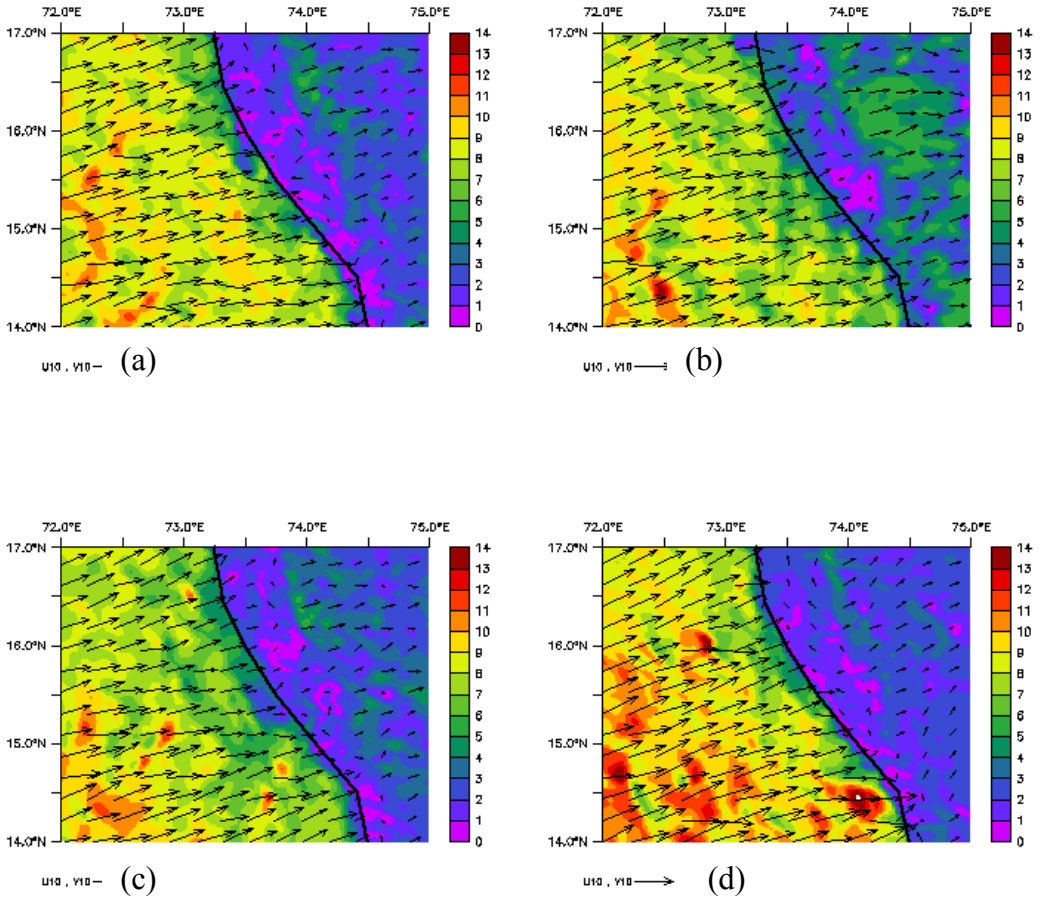

Fig. 10 Simulated high resolution surface in the Goa region at (a) 0530 h, (b) 1330 h, (c)1730 h, and (d) 2130 h respectively on 17 July 2006

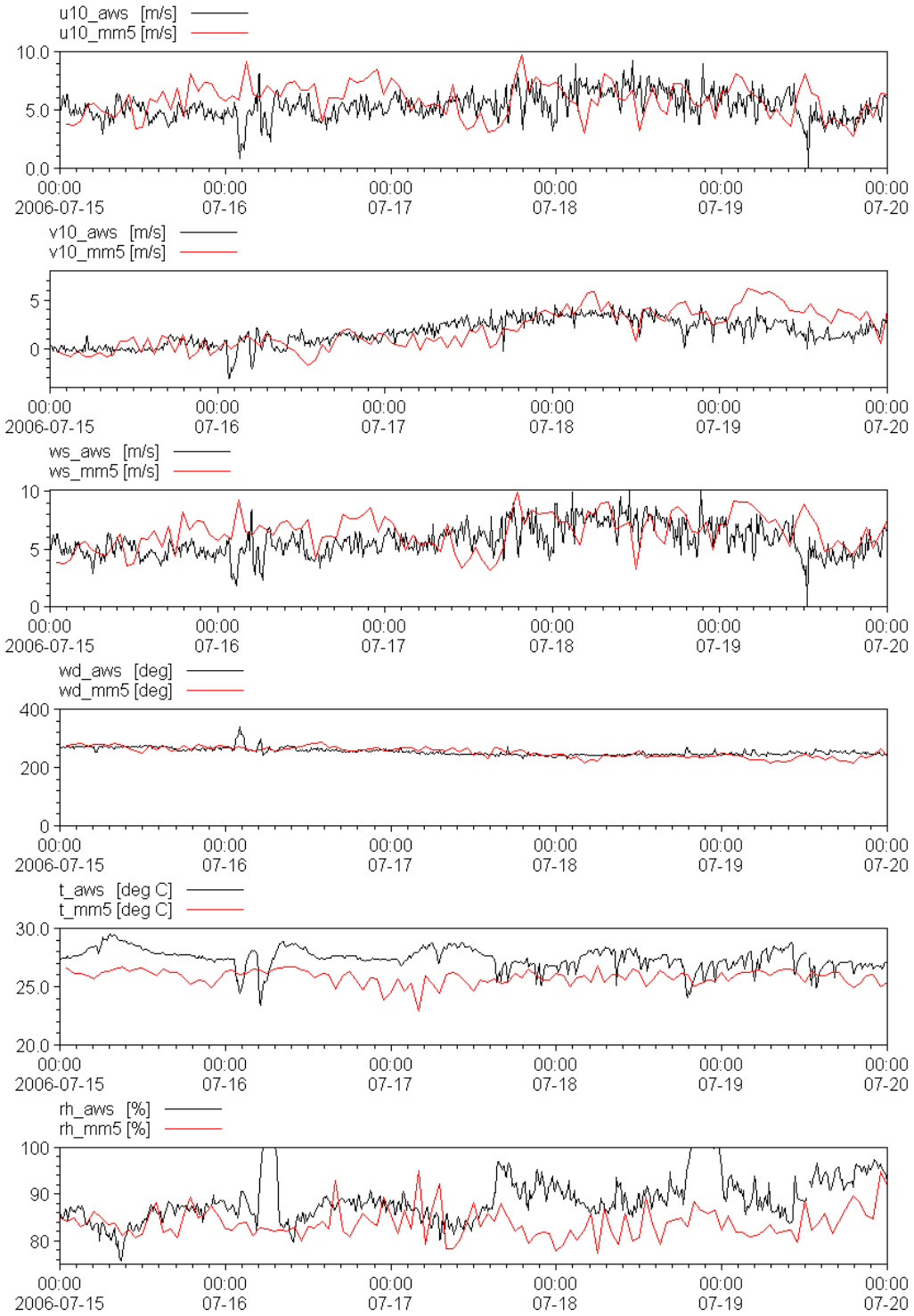

Fig. 11 Comparison of simulated and AWS observed (a) u-velocity component at 10m height, (b) v-velocity component at 10m height, (c) wind speed and (d) wind direction, , (e) air temperature and (f) relative humidity (time in UTC) of July 2006

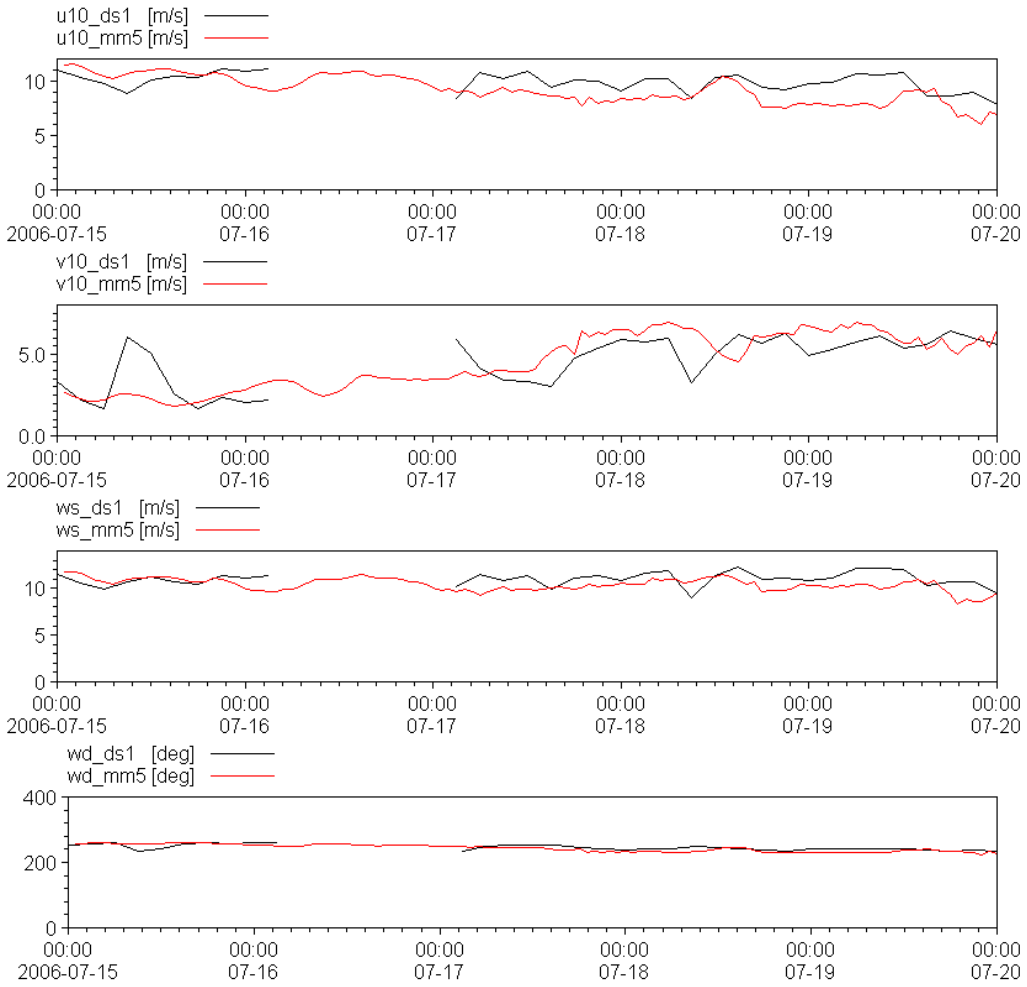

Fig. 12 Comparison of simulated and moored buoy (SW3) observations (a) u-velocity component at 10m height, (b) v-velocity component at 10m height, (c) wind speed and (d) wind direction (time in UTC) of July 2006

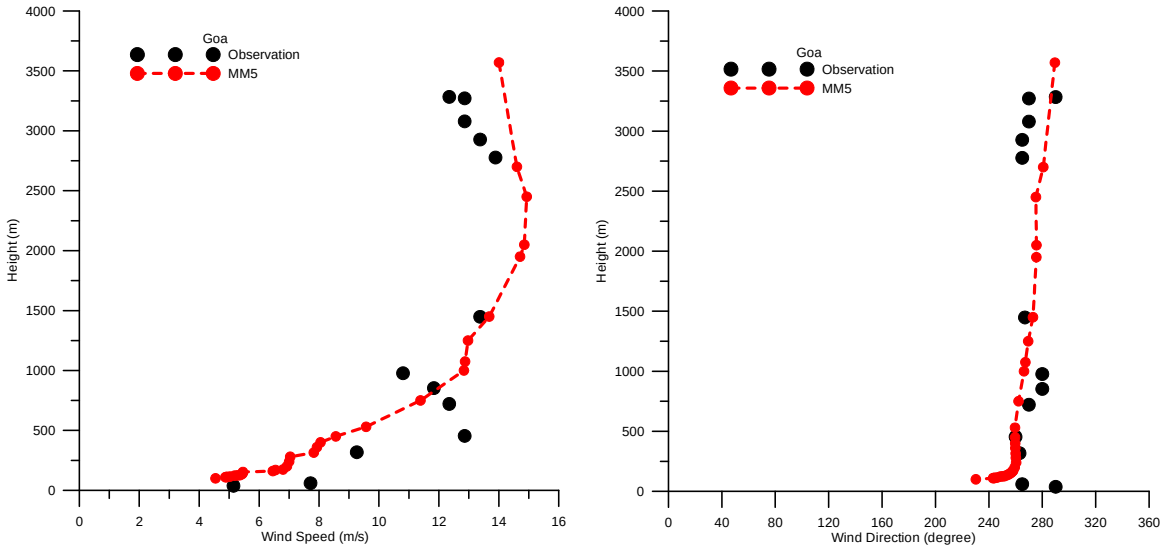

Fig. 13 Comparison of simulated and observed vertical profile of (a)wind speed at 00GMT and (b) wind direction at 00 GMT of 17 July 2006

Table I. Detail of grids and physics options used in the MM5 model

Dynamics	Primitive equation, non-hydrostatic		
Vertical resolution	23 σ levels		
Horizontal resolution	27 km	9km	3km
Domains of integration	65.8ºE-81.8 ºE	68.8 ºE-78.8 ºE	71.8 ºE-75.8ºE
	7.45 ºE-23.45 ºE	10.45 ºE-20.45 ºE	13.45 ºE-17.45ºE
Radiation	Rapid radiation transfer model (RRTM) for long wave		
radiation			
Surface processes	Five-layer soil model		
Planetary boundary layer	MRF PBL		
Convection	Grell scheme		
Explicit moisture	Simple ice (SI) scheme		

Table II. Statistical parameters of hourly MM5 surface wind simulations and AWS measurements for different seasons

	Bias (m/s)	Standard Deviation (m/s)	RMSE (m/s)	Correlation Coefficient
NE monsoon	$u_{10\,(aws)}$ =-0.37 $v_{10(aws)}$ = 0.41	$u_{10\,(aws)}$ = 1.591 $v_{10(aws)}$ = 0.9987	$u_{10\,(aws)}$ =1.269 $v_{10(aws)}$ = 1.261	$u_{10\,(aws)}$ =0.7337 $v_{10(aws)}$ = 0.631
Transition period	$u_{10\,(aws)}$ =0.1619 $v_{10(aws)}$ =0.318	$u_{10\,(aws)}$ =1.8709 $v_{10(aws)}$ =0.921	$u_{10\,(aws)}$ =1.129 $v_{10(aws)}$ =1.004	$u_{10\,(aws)}$ =0.8419 $v_{10(aws)}$ =0.6512
SW monsoon	$u_{10\,(aws)}$ =0.1342 $v_{10(aws)}$ =0.431	$u_{10\,(aws)}$ =1.824 $v_{10(aws)}$ =0.901	$u_{10\,(aws)}$ =1.201 $v_{10(aws)}$ =1.12	$u_{10\,(aws)}$ =0.703 $v_{10(aws)}$ =0.602